energies

MDPI

Article

Doping-Induced Isotopic $Mg^{11}B_2$ Bulk Superconductor for Fusion Application

Qi Cai [1], Qianying Guo [1], Yongchang Liu [1,*], Zongqing Ma [1,2], Huijun Li [1], Wenbin Qiu [2], Dipak Patel [2], Hyunseock Jie [2], Jung Ho Kim [2], Mehmet Somer [3], Ekrem Yanmaz [4], Arnaud Devred [5], Vladimir Luzin [6], Amanullah Fatehmulla [7], Wazirzada Aslam Farooq [7], Daniel Gajda [8], Yoshio Bando [9], Yusuke Yamauchi [2,9], Subrata Pradhan [10] and Md. Shahriar A. Hossain [2,9,*]

1 State Key Lab of Hydraulic Engineering Simulation and Safety, School of Materials Science & Engineering, Tianjin University, Tianjin 300072, China; caiqi6406608@163.com (Q.C.); qyguo@tju.edu.cn (Q.G.); zqma@uow.edu.au (Z.M.); huijun@uow.edu.au (H.L.)
2 Institute of Superconducting and Electronic Materials, Australian Institute for Innovative Materials (AIIM), University of Wollongong, Squires Way, North Wollongong, NSW 2500, Australia; wq118@uowmail.edu.au (W.Q.); djp485@uowmail.edu.au (D.P.); hj867@uowmail.edu.au (H.J.); jhk@uow.edu.au (J.H.K.); yusuke@uow.edu.au (Y.Y.)
3 Chemistry Department, Koc University, Rumelifeneri Yolu, Sariyer-Istanbul TR-34450, Turkey; msomer@ku.edu.tr
4 Department of Mechatronics, Faculty of Engineering and Architecture, Gelisim University, Istanbul 34315, Turkey; eyanmaz@gelisim.edu.tr
5 International Thermonuclear Experimental Reactor (ITER) Organization, 13115 Saint Paul Lez Durance, France; arnaud.devred@iter.org
6 Australian Nuclear Science and Technology Organization (ANSTO), Lucas Heights, NSW 2232, Australia; vll@ansto.gov.au
7 Department of Physics and Astronomy, College of Science, King Saud University, Riyadh 11451, Saudi Arabia; aman@ksu.edu.sa (A.F.); wafarooq@hotmail.com (W.A.F.)
8 International Laboratory of High Magnetic Fields (HMF) and Low Temperatures (LT), Gajowicka 95, 53-421 Wroclaw, Poland; dangajda@op.pl
9 International Center for Materials Nanoarchitectonics (MANA), National Institute for Materials Science (NIMS) 1-1 Namiki, Tsukuba, Ibaraki 305-0044, Japan; bando.yoshio@nims.go.jp
10 Institute for Plasma Research, Bhat, Gandhinagar 382 428, Gujarat, India; subrata.s.pradhan@gmail.com
* Correspondence: ycliu@tju.edu.cn (Y.L.); shahriar@uow.edu.au (M.S.A.H.); Tel.: +86-22-8535-6735 (Y.L.); +61-2-4221-3384 (M.S.A.H.)

Academic Editors: Matthew Hole and Tapas Mallick
Received: 2 November 2016; Accepted: 10 March 2017; Published: 21 March 2017

Abstract: Superconducting wires are widely used for fabricating magnetic coils in fusion reactors. Superconducting magnet system represents a key determinant of the thermal efficiency and the construction/operating costs of such a reactor. In consideration of the stability of ^{11}B against fast neutron irradiation and its lower induced radioactivation properties, MgB_2 superconductor with ^{11}B serving as the boron source is an alternative candidate for use in fusion reactors with a severe high neutron flux environment. In the present work, the glycine-doped $Mg^{11}B_2$ bulk superconductor was synthesized from isotopic ^{11}B powder to enhance the high field properties. The critical current density was enhanced (10^3 A·cm^{-2} at 20 K and 5 T) over the entire field in contrast with the sample prepared from natural boron.

Keywords: MgB_2 superconductor; isotope ^{11}B; transition temperature; critical current density

1. Introduction

Fusion power is one of the most promising energy source candidates to solve global energy problems, considering its safety and green merits compared with conventional mineral energy sources. In the world-class International Thermonuclear Experimental Reactor (ITER) fusion energy project, the superconducting magnet system serves as a key determinant (Figure 1). A high and steady magnetic field needs to be produced to confine the deuterium (D)–tritium (T) burning plasma inside the ITER Tokamak nuclear fusion reactor. According to the previous ITER plan, hundreds of tons of superconducting cables made from NbTi and Nb_3Sn strands have been fabricated to assemble 18 Nb_3Sn toroidal field (TF) coils, a 6-module Nb_3Sn central solenoid (CS) coil, six Nb-Ti poloidal field (PF) coils, and nine pairs of Nb-Ti correction coils (CC) [1–3]. ITER is aimed at demonstrating the feasibility of fusion energy, but for the next step, the development of a commercial fusion reactior there is a concern that, after irradiation, ^{93}Nb be transformed into the long-lived nuclide ^{94}Nb with a half-life of about 20,000 years [4,5]. Hence, coil maintenance and repairs may become more cumbersome and the recycling of irradiated Nb-based alloys may call for tens of thousands of years of waiting for them to "cool down". Meanwhile, thicker shielding will be necessary for long-term operation. For the convenience of radioactive waste treatment and environmental protection, the radioactivation properties of superconducting components within the fusion reactor should be taken into account. The superconductivity of MgB_2 was discovered in 2001 [6]. It is well-known for its simple binary chemical composition and much higher critical transition temperature (T_c) of 39 K than that of NbTi at 9.3 K. In order to operate Nb-based low-temperature superconductors, the core of the magnet needs to be cooled down to 4 K. The only eligible cryogen is liquid helium, which is extremely expensive, not always available, and very difficult to handle. In the case of MgB_2, a working temperature as high as 20 K is low enough to achieve acceptable performance. Remarkably, the operating cost is expected to be cut by over 50% by substituting cryocooler-cooled MgB_2 materials at 20 K for liquid-helium-cooled Nb-based superconductors. Therefore, due to the advantages of cost-effectiveness, lower radioactivation, and the shorter decay time of isotopic $Mg^{11}B_2$, fundamental research on $Mg^{11}B_2$ superconducting wires will be valuable for improving the efficiency of practical application in high-irradiation environments such as fusion reactors. Nevertheless, the application of the un-doped MgB_2 remains limited by the sensitivity of the critical current density (J_c) to the increasing applied magnetic field [7]. By yielding an enhancement of J_c especially at high field, chemical doping enabled MgB_2 to meet higher demand in practical application, and carbon-containing compounds definitely attracted the most attention within the dopant's family.

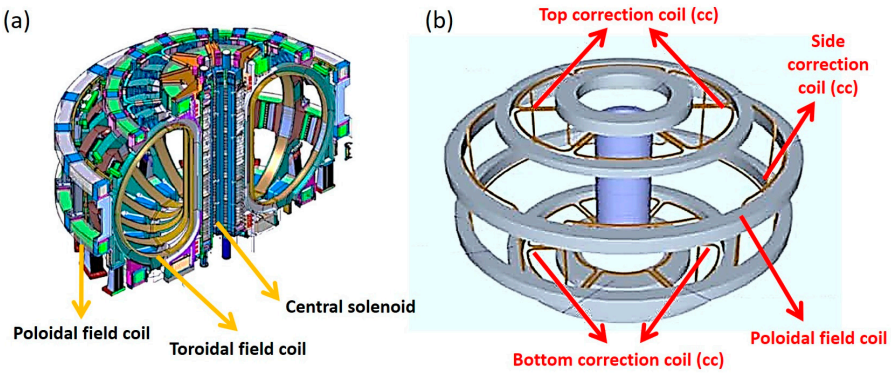

Figure 1. (**a**) 3D illustration of superconducting magnet consisting of poloidal field (PF), toroidal field (TF), and central solenoid (CS) coils; and (**b**) replaceable parts with MgB_2 [1,2].

MgB_2 bulks and wires with carbon addition, for instance, malic acid [8], graphene, coronene, or glucose [9–11], have been under investigation, motivated by the potential response of carbon atoms (compared to boron) to donate their additional valence electrons to the σ conduction band.

Glycine ($C_2H_5NO_2$, Glycine) was doped into MgB_2 bulks by a series of techniques in our previous study [12,13]. The dominating mechanism for the enhancement of the J_c lied in the MgO formation in advance of the Mg-B solid-solid reaction, and the simultaneously released carbon atoms provided a certain contribution as well, by substitution the B sites in the MgB_2 lattice. Apart from the carbon doping method, a new trial related to the state of the boron precursor has been carried out as well. The MgB_2 wires prepared from laboratory made nano-sized boron achieved the J_c of 10^5 A·cm^{-2} at 5 K and 4 T [14]. Bovone et al. [15] produced boron powder by magnesiothermic reduction of boron oxide in the lab, which proved to be an excellent precursor for MgB_2 wire manufacture independent of the applied technique. Furthermore, commercial carbon-coated amorphous boron powder brought along carbon doping and benefited the J_c of the synthesized MgB_2 bulks with or without Cu doping [16,17].

Considering the type of the original boron powder, isotopic boron has been adopted to determine the effect on the superconductivity and physical properties of MgB_2. The studies of both Bud'ko et al. [18] and Hinks et al. [19] indicated a difference of 1 K in transition temperature (T_c) for the un-doped MgB_2 made of ^{10}B and ^{11}B. Simonelli et al. [20] investigated the isotope effect on phonon spectra of MgB_2 with Al doping and suggested a difference in Raman shift for the two isotopic forms of MgB_2. Recently, Alarco et al. [21] extended the study to the effect of ^{10}B, ^{11}B and natural B (mixture of ^{10}B and ^{11}B) on the phonon frequencies, which exhibited a pronounced isotopic effect for the phonon modes. Compared with conventional Nb-based superconductors, MgB_2 features "low activation" and a much shorter decay time. Within 1 year, the dose rate of MgB_2 materials will be reduced to the hands-on maintenance level, which is desirable for a fusion reactor magnet system [4]. Additionally, because of the reaction $^{10}B + n \rightarrow {}^{7}Li + He$ (gas) under the heavy irradiation condition, ^{10}B can no longer guarantee the stability of the MgB_2 superconducting magnet. ^{10}B isotope is transformed to ^{7}Li and He by the neutron irradiation, while ^{11}B isotope is stable against the neutron irradiation without nuclear transformation and can reduce nuclear heating from 2.58 to 0.13 W/cm^3 [22].

By replacing ^{10}B with the isotope ^{11}B, $Mg^{11}B_2$ superconducting wires will be much more stable in a neutron irradiation environment due to the smaller neutron capture cross-section of ^{11}B [23]. Considering the abundant reserves of ^{11}B on Earth (20 wt % for ^{10}B, 80 wt % for ^{11}B), the anticipated cost for extracting the isotope from natural boron is expected to be reduced during the chemical synthesis. Mg $^{11}B_2$ would be a promising candidate material as a lower field poloidal field and correction coil superconducting magnets in a fusion reactor (Figure 1). In view of this, glycine-doped MgB_2 bulks are prepared from natural B (written as $^{10.8}B$) and ^{11}B in this study to improve the critical current density at high field region.

2. Experimental Details

Amorphous $^{10.8}B$ (93%–94% purity, 0.6–0.7 μm in size) or ^{11}B powder (amorphous, 99.2% in purity, about 5 μm in size, from Pavezyum Kimya, Istanbul, Turkey), Mg powder (99.5% purity, 100 μm in size), and glycine powder (99% purity) were mixed in the ratio of MgB_2 + 3 wt % Gly. After ground thoroughly in an agate mortar, the mixture was pressed into cylindrical pellets (5 mm diameter and 1.5 mm thickness) under a pressure of 5 MPa. The obtained pellets were then sintered in the differential thermal analysis apparatus (DSC 404C, Netzsch, Boston, MA, USA) at 800 °C for 0.5 h with a heating rate of 10 °C·min^{-1} and a cooling rate of 40 °C·min^{-1}. The whole process was accomplished under the protection of flowing high-purity Ar gas. The superconducting properties were measured on a superconducting quantum interference device (SQUID–VSM, Quantum Design, San Diego, CA, USA) after the sample was cut into a slab ($4 \times 2 \times 1$ mm^3). The corresponding J_c values were calculated from the width of magnetization hysteresis loops based on the Bean model $J_c = 20\Delta M/[a/(1 - a/3b)]$ [24], where M is the volume magnetization, ΔM is the difference in volume magnetization between the arms of the M–H loop, and a and b are the sample dimensions ($a < b$).

3. Results and Discussion

Analogous to the un-doped and the Gly-doped $Mg^{10.8}B_2$, the Gly-doped $Mg^{11}B_2$ is composed of MgB_2 as the main phase and MgO as the only impurity phase (Figure 2).

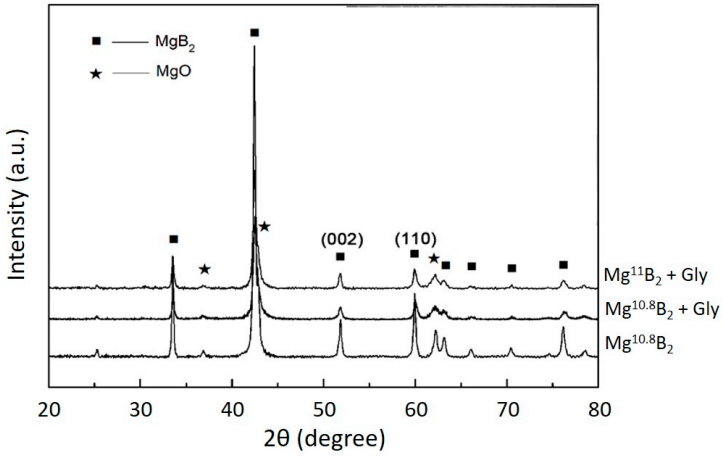

Figure 2. X–ray diffraction patterns for the un-doped $Mg^{10.8}B_2$, the Gly-doped $Mg^{10.8}B_2$, and the Gly-doped $Mg^{11}B_2$ samples.

Generally, doping from carbon sources results in the substitution of carbon for boron in the MgB_2 lattice. Substituted carbon atoms normally donate their additional valence electrons (compared to boron) to the σ conduction band, resulting in decreased carrier concentration by filling the holes and decreasing the superconducting gaps. This will reduce the number of holes at the top of the σ bands together with a reduction of the electronic density of states [25], and consequently the transition temperature T_c was supposed to decrease. Previous studies have stated that the MgB_2 samples showed a strong boron isotope effect, as the T_c for $Mg^{11}B_2$ decreased almost 1 K in contrast with the $Mg^{10}B_2$ sample [18,19]. However, the T_c for the Gly-doped $Mg^{11}B_2$ sample remained at the same level as the doped $Mg^{10.8}B_2$ sample shown in Figure 3.

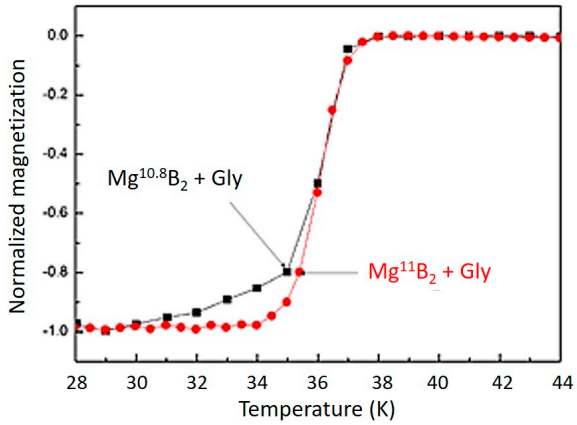

Figure 3. Temperature dependence of normalized magnetization for the Gly-doped $Mg^{10.8}B_2$ and the Gly-doped $Mg^{11}B_2$ samples.

From the viewpoint of the isotope effect, the increase of the phonon frequency is conductive to improve T_c, and the approach of the phonon and coulomb energies will lead to a decrease of T_c. As summarized by Knigavko [26], the T_c would remain stable when the two effects reached a balance in the Gly-doped $Mg^{11}B_2$ sample. The replaced carbon atoms likely originated from the reaction of

Mg and the decomposition product of glycine, $2Mg + CO_2 \rightarrow C + 2MgO$, with the impurity phase MgO generated. Contrary to the common position that the dielectric MgO occupied in most doping systems, i.e., at the grain boundary [27], the MgO particles in the Gly-doped $Mg^{11}B_2$ sample might be embedded within the MgB_2 grains in the nano-scale dimension. Besides, element mappings for Mg and O on an area with holes are shown in Figure 4a–c. Combined with the distribution of Mg element, the MgO phase was believed to be dispersed homogeneously on the matrix rather than gathered in the hole, which implied good MgB_2 grain connectivity. A thermodynamic calculation has demonstrated that the MgO phase was formed prior to MgB_2, and the study on undoped $Mg^{11}B_2$ suggested that the ^{11}B accelerated the Mg-B solid-solid reaction below 650 °C [28]. Hence, the MgO particles were mostly included in the growing MgB_2 grains instead of aggregating at the boundary. The size and distribution of MgO allowed them to become effective pinning centers, and as a result, the Gly-doped sample had a significantly improved J_c performance at least twice larger than those of pure MgB_2 over the entire field at 20 K. The measured J_c-H characteristics of the un-doped and the Gly-doped samples at 20 K are illustrated in Figure 4d. A further improvement in J_c was observed in the Gly-doped $Mg^{11}B_2$ sample, even at the low field. The enhanced J_c should be attributed to the use of high-purity ^{11}B powder as well, in view that Gly-doped sample prepared from high-purity boron shows two times higher J_c than that from low-purity boron powder [29].

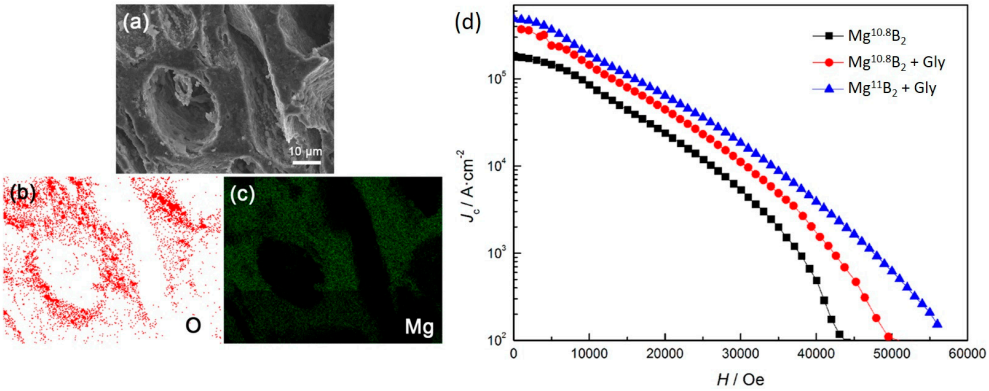

Figure 4. (**a**) Scanning electron microscopy (SEM) image; (**b**,**c**) corresponding element mappings of O and Mg for the Gly-doped $Mg^{11}B_2$ sample; and (**d**) Measured J_c-H characteristics at 20 K for the un-doped $Mg^{10.8}B_2$, the Gly-doped $Mg^{10.8}B_2$, and the Gly-doped $Mg^{11}B_2$ samples.

4. Conclusions

A glycine-doped $Mg^{11}B_2$ sample with layered grains was synthesized from isotopic ^{11}B powder. The glycine-doped $Mg^{11}B_2$ gives comparable critical current density and could be used for fusion reactors because of endurance against neutron irradiation. The results obtained in this work could guide the fabrication of $Mg^{11}B_2$ wires to be used as magnet coils in fusion reactor systems such as ITER-type tokamak magnets.

Acknowledgments: The authors are grateful to the China National Funds for Distinguished Young Scientists (Granted No. 51325401), the National High Technology Research and Development Program of China (Granted No. 2015AA042504) for grant and financial support. The authors also extend their appreciation to the International Scientific Partnership Program (ISPP) at King Saud University for funding this research work through ISPP-0066. This work is partially supported by the Australian Research Council (Grant No. DE140101333). Funding for the Australia-India Early Career Researcher Fellowship was provided to Md. Shahriar A. Hossain in 2017 by the Australian Academy of Science, on behalf of the Australian Government Department of Industry, Innovation and Science to work with Subrata Pradhan. Further Subrata Pradhan acknowledges Department of Atomic Energy Scientific Research Council (DAE-SRC), Government of India Grant bearing sanction number 21/10/2015-BRNS with DAESRC, BRNS.

Author Contributions: Qi Cai, Zongqing Ma, Md. Shahriar A. Hossain and Yongchang Liu designed the experiments. Qi Cai, Qianying Guo, Wenbin Qiu, Dipak Patel, Hyunseock Jie, Vladimir Luzin and Daniel Gajda performed the experiments. Huijun Li, Mehmet Somer, Ekrem Yanmaz, Subrata Pradhan,

Yongchang Liu, Jung Ho Kim and Md. Shahriar A. Hossain contributed material characterizations. Qi Cai, Md. Shahriar A. Hossain, Huijun Li, Mehmet Somer, Ekrem Yanmaz, Arnaud Devred, Subrata Pradhan, Yusuke Yamauchi, Yoshio Bando, Amanullah Fatehmulla and Wazirzada Aslam Farooq analyzed the data.

Conflicts of Interest: The authors declare no conflict of interest.

Disclaimer: The views and opinions expressed herein do not necessarily reflect those of the ITER Organization.

References

1. Mitchell, N.; Bessette, D.; Gallix, R.; Jong, C.; Knaster, J.; Libeyre, P.; Sborchia, C.; Simon, F. The ITER Magnet System. *IEEE Trans. Appl. Supercond.* **2008**, *18*, 435–440. [CrossRef]
2. Salpietro, E. Status of the ITER magnets. *Supercond. Sci. Technol.* **2006**, *19*, S84. [CrossRef]
3. Devred, A.; Backbier, I.; Bessette, D.; Bevillard, G.; Gardner, M.; Jong, C.; Lillaz, F.; Mitchell, N.; Romano, G.; Vostner, A. Challenges and status of ITER conductor production. *Supercond. Sci. Technol.* **2014**, *27*, 044001. [CrossRef]
4. Noda, T.; Takeuchi, T.; Fujita, M. Induced activity of several candidate superconductor materials in a tokamak-type fusion reactor. *J. Nucl. Mater.* **2004**, *329–333*, 1590–1593. [CrossRef]
5. Noda, T.; Maki, K.; Takeuchi, T.; Suzuki, H.; Araki, H.; Yang, W. Induced activity and damage of superconducting materials for a fusion reactor. *Fusion Eng. Des.* **2006**, *81*, 1033–1037. [CrossRef]
6. Nagamatsu, J.; Nakagawa, N.; Muranak, T.; Zenitani, Y.; Akimitsu, J. Superconductivity at 39 K in magnesium diboride. *Nature* **2001**, *410*, 63–64. [CrossRef] [PubMed]
7. Finnemore, D.K.; Ostenson, J.E.; Bud'ko, S.L.; Lapertot, G.; Canfield, P.C. Thermodynamic and transport properties of superconducting (MgB_2)-B-10. *Phys. Rev. Lett.* **2001**, *86*, 2420. [CrossRef] [PubMed]
8. Hossain, M.S.A.; Senatore, C.; Flukiger, R.; Rindfleisch, M.A.; Tomsic, M.J.; Kim, J.H.; Dou, S.X. The enhancement of Jc and Birr of in-situ MgB_2 wires and tapes alloyed with $C_4H_6O_5$ (malic acid) after cold high pressure densification. *Supercond. Sci. Technol.* **2009**, *22*, 095004. [CrossRef]
9. De Silva, K.S.B.; Xu, X.; Gambir, S.; Wong, D.C.; Li, W.; Hu, Q.Y. Effect of sintering temperature on the superconducting properties of graphene doped MgB_2. *IEEE Trans. Appl. Supercond.* **2013**, *23*, 7100604. [CrossRef]
10. Ye, S.J.; Matsumoto, A.; Zhang, Y.C.; Kumakura, H. Strong enhancement of high-field critical current properties and irreversibility field of MgB_2 superconducting wires by coronene active carbon source addition via the new B powder carbon-coating method. *Supercond. Sci. Technol.* **2014**, *27*, 085012. [CrossRef]
11. Hossain, M.S.A.; Kim, J.H.; Wang, X.L.; Xu, X.; Peleckis, G.; Dou, S.X. Enhancement of flux pinning in a MgB_2 superconductor doped with tartaric acid. Supercond. *Sci. Technol.* **2007**, *20*, 112.
12. Cai, Q.; Ma, Z.; Liu, Y.; Yu, L. Enhancement of critical current density in glycine-doped MgB_2 bulks. *Mater. Chem. Phys.* **2012**, *136*, 778. [CrossRef]
13. Cai, Q.; Liu, Y.; Ma, Z.; Yu, L. Significant enhancement of critical current density in Gly-doped MgB_2 bulk by tailoring the formation of MgO. *Scr. Mater.* **2012**, *67*, 92. [CrossRef]
14. Vignolo, M.; Bovone, G.; Matera, D.; Nardelli, D.; Bernini, C.; Siri, A.S. Nano-sized boron synthesis process towards the large scale production. *Chem. Eng. J.* **2014**, *256*, 32. [CrossRef]
15. Bovone, G.; Matera, D.; Bernini, C.; Magi, E.; Vignolo, M. Manufacturing process influence on superconducting properties of MgB_2 wires prepared using laboratory made boron. *Supercond. Sci. Technol.* **2015**, *28*, 065006. [CrossRef]
16. Barua, S.; Hossain, A.; Shahriar, M.; Ma, Z. Superior critical current density obtained in MgB_2 bulks through low-cost carbon-encapsulated boron powder. *Scr. Mater.* **2015**, *104*, 37. [CrossRef]
17. Liu, Y.; Lan, F.; Ma, Z.; Chen, N.; Li, H.; Barua, S.; Patel, D.; Shahriar, M.; Hossain, A.; Acar, S. Significantly enhanced critical current density in nano- MgB_2 grains rapidly formed at low temperature with homogeneous carbon doping. *Supercond. Sci. Technol.* **2015**, *28*, 55005. [CrossRef]
18. Bud'ko, S.L.; Lapertot, G.; Petrovic, C.; Cunningham, C.E.; Anderson, N.; Canfield, P.C. Boron isotope effect in superconducting MgB_2. *Phys. Rev. Lett.* **2001**, *86*, 1877. [CrossRef] [PubMed]
19. Hinks, D.; Claus, H.; Jorgensen, J. The complex nature of superconductivity in MgB_2 as revealed by the reduced total isotope effect. *Nature* **2001**, *411*, 457. [CrossRef] [PubMed]

20. Simonelli, L.; Palmisano, V.; Fratini, M.; Filippi, M.; Parisiad es, P.; Lampakis, D.; Liarokapis, E.; Bianconi, A. Isotope effect on the E-2g phonon and mesoscopic phase seperation near the electronic topological transition in $Mg_{1-x}Al_xB_2$. *Phys. Rev. B* **2009**, *80*, 014520. [CrossRef]
21. Alarco, J.A.; Talbot, P.C.; Mackinnon, I.D. Coherent phonon decay and the boron isotope effect for MgB_2. *Phys. Chem. Chem. Phys.* **2014**, *16*, 25386. [CrossRef] [PubMed]
22. Hishinuma, Y.; Kikuchi, A.; Shimada, Y.; Kashiwai, T.; Hata, S.; Yamada, S.; Muroga, T.; Sagara, A. Development of MgB_2 superconducting wires for the low activation superconducting magnet system operated around core D-T plasma. *Fusion Eng. Des.* **2015**, *98–99*, 1076. [CrossRef]
23. Mooring, F.P.; Monahan, J.E.; Huddleston, C.M. Neutron cross sections of boron isotopes for energies between 10 and 100 KeV. *Nucl. Phys.* **1966**, *82*, 16–32. [CrossRef]
24. Bean, C.P. Magnetization of hard superconductors. *Phys. Rev. Lett.* **1962**, *8*, 250. [CrossRef]
25. Kortus, J.; Dolgov, O.V.; Kremer, R.K.; Golubov, A.A. Band filling and interband scattering effects in MgB_2: Carbon versus aluminium doping. *Phys. Rev. Lett.* **2005**, *94*, 027002. [CrossRef] [PubMed]
26. Knigavko, A.; Marsiglio, F. Constraints from T_c and the isotope effect in MgB_2. *Phys. Rev. B* **2001**, *64*, 172513. [CrossRef]
27. Ma, Z.Q.; Liu, Y.C.; Gao, Z.M. The synthesis and grain connectivity of lamellar MgB_2 grains by Cu-activated sintering at low temperature. *Scr. Mater.* **2010**, *63*, 399–402. [CrossRef]
28. Cheng, F.; Liu, Y.; Ma, Z.; Li, H.; Hossain, M.S.A. Superior Critical current density obtained in $Mg^{11}B_2$ low activation superconductor by using reactive amorphous ^{11}B and optimizing sintering temperature. *J. Alloys Compd.* **2015**, *650*, 508. [CrossRef]
29. Wu, F.; Cai, Q. Comparison of critical current density in undoped, glycine doped and Cu-and-glycine-co-doped MgB_2 synthesized from nm-Boron and μm-Boron. *J. Supercond. Nov. Magn.* **2014**, *27*, 2023–2027. [CrossRef]